

Borane-Catalyzed C–F Bond Functionalization of *gem*-Difluorocyclopropenes Enables the Synthesis of Orphaned Cyclopropanes

Joseph P. Mancinelli, Wang-Yeuk Kong, Wentao Guo, Dean J. Tantillo, and Sidney M. Wilkerson-Hill*



Cite This: *J. Am. Chem. Soc.* 2023, 145, 17389–17397



Read Online

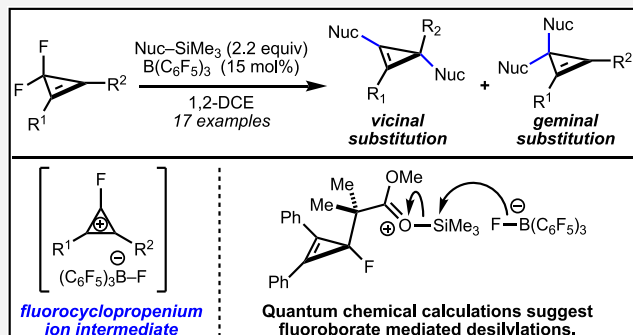
ACCESS |

Metrics & More

Article Recommendations

Supporting Information

ABSTRACT: Herein, we disclose an approach to synthesize *tert*-alkyl cyclopropanes by leveraging C–F bond functionalization of *gem*-difluorocyclopropenes using tris(pentafluorophenyl)borane catalysis. The reaction proceeds through the intermediacy of a fluorocyclopropenium ion, which was confirmed by the isolation of $[\text{Ph}_2(\text{C}_6\text{D}_5)\text{C}_3]^+[(\text{C}_6\text{F}_5)_3\text{BF}]^-$. We found that silylketene acetal nucleophiles were optimal reaction partners with fluorocyclopropenium ion intermediates yielding fully substituted cyclopropenes functionalized with two α -*tert*-alkyl centers (63–93% yield). The regioselectivity of the addition to cyclopropenium ions is controlled by their steric and electronic properties and enables access to 3,3-bis(difluoromethyl)cyclopropenes in short order. The resulting cyclopropene products are readily reduced to the corresponding orphaned cyclopropanes under hydrogenation conditions. Quantum chemical calculations reveal the nature of the C–F bond cleavage steps and provide evidence for catalysis by boron and not silylated oxonium ions, though Si–F bond formation is the enthalpic driving force for the reaction.



Downloaded via UNIV OF CALIFORNIA DAVIS on September 15, 2023 at 16:51:57 (UTC).
See https://pubs.acs.org/sharingguidelines for options on how to legitimately share published articles.

INTRODUCTION

Cyclopropanes are a class of carbocycles often employed in drug development because of their unique physical properties. The geometry, strain, and bonding modes of this motif impart higher metabolic stabilities, binding affinities, and lipophilicity *in vivo* relative to acyclic analogues.¹ The success of cyclopropane-containing drugs is best exemplified by antiviral molecules such as beclabuvir,² lenacapavir,³ and nirmatrelvir,⁴ compounds used to treat HCV-1, HIV-1, and SARS-CoV-2, respectively.

Oxidation of cyclopropylmethyl (CM) groups is a metabolic process that clears drugs from cells.⁵ Thus, methods to obtain cyclopropanes containing functionality that blocks oxidation at the CM position (e.g., by the incorporation of quaternary carbons or fluorine atoms) would be welcomed in drug discovery (Figure 1). These *tert*-alkylcyclopropanes⁶ and fluorinated cyclopropanes are largely unobtainable using common cyclopropanation methods⁷ like Simmons–Smith reactions⁸ or metal-catalyzed diazo decomposition⁹ due to the steric bulk and unwanted side reactivity of metal carbenoids.¹⁰ Additionally, direct functionalization reactions of the CM groups often result in rapid ring opening *via* cationic, radical, and transition-metal-mediated processes,¹¹ making this disconnection unviable. Thus, they have been “orphaned” or left behind by traditional cyclopropanation methodologies.

As a part of a research program aimed at developing routes to the synthesis of “orphaned” cyclopropanes,¹² we sought to develop a new substitution reaction of cyclopropenes as a strategy to obtain highly congested *tert*-alkylcyclopropane carbocycles. *gem*-Difluorocyclopropenes have emerged as attractive candidates for the proposed substitution reaction because of their ease of synthesis,¹³ well-documented physical properties,¹⁴ and reactivity.¹⁵ We hypothesized that catalytic C–F bond functionalization of difluorocyclopropenes could be achieved based on studies conducted by Sargeant, West, and Smart, which demonstrated that fluorocyclopropenium ions are readily obtained from tetrafluorocyclopropenes by fluoride ion abstraction using SbF_5 or $\text{BF}_3\text{-OEt}_2$.¹⁶ Furthermore, Breslow and co-workers reported the addition of Grignard reagents to cyclopropenium perchlorates,¹⁷ thus demonstrating the feasibility of C–C bond-forming reactions from cyclopropenium ion intermediates.¹⁸ The successful orchestration of these elementary steps (*i.e.*, C–F bond cleavage and C–C bond formation) would result in a net substitution reaction

Received: May 20, 2023

Published: July 26, 2023



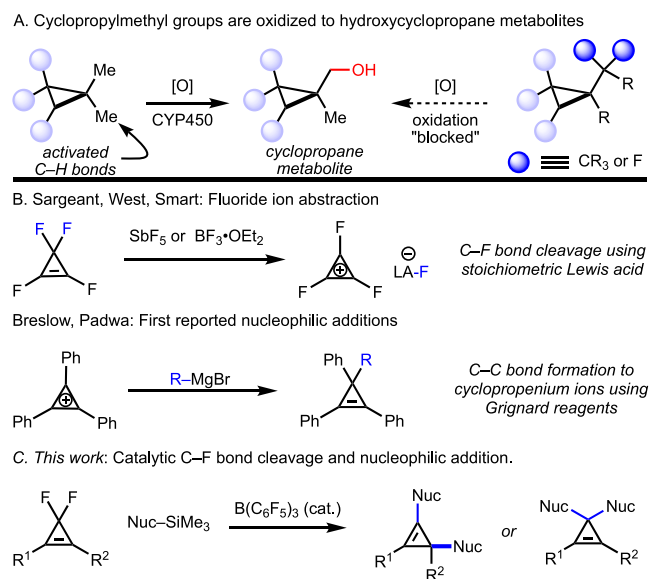


Figure 1. (A) Oxidation at the CM position results in hydroxylated cyclopropane metabolites. Proposed strategy to block oxidation with quaternary carbons or fluorination. (B) Seminal reports in fluorocyclopropenium ion generation and cyclopropenium ion reactivity. (C) Proposed reaction for this study.

analogous to those published by Corey and Posner¹⁹ on dibromocyclopropane derivatives. The proposed C–F bond functionalization of difluorocyclopropenes stands in direct contrast to carbometallation²⁰ and hydrogenation²¹ reactions of cyclopropenes, which functionalize the C–C double bond of cyclopropenes by virtue of strain, and provides an avenue to overcome deleterious ring-opening reactions of the highly reactive intermediates formed in such reactions.

RESULTS AND DISCUSSION

We began these studies by testing the ability of electron-deficient boranes²² to activate the C–F bonds of difluorocyclopropenes because of their high Lewis acidity^{23,24} and their established fluoride ion affinities.²⁵ In addition, several reports have demonstrated the ability of boranes to cleave C–F bonds in fluoroalkanes.^{26–33} Upon combining stoichiometric amounts of cyclopropene **1** (1.0 equiv) and $B(C_6F_5)_3$ (1.0 equiv) in C_6D_6 (0.7 mL), white needles spontaneously crystallized from the solution over 2 h. X-ray crystallographic

analysis of a single crystal of this solid revealed it to be d_5 -triphenylcyclopropenium tris(pentafluorophenyl)fluoroborate ($[Ph_2(C_6D_5)C_3]^+[C_6F_5)_3BF]^-,$ **3**) (45% isolated yield) (Scheme 1).³⁴ Presumably, the salt arose from a Friedel–Crafts addition of C_6D_6 to fluorodiphenylcyclopropenium ion (**4**) generated *in situ* and then a second C–F bond functionalization from intermediate **6**. This exciting discovery not only demonstrates that $B(C_6F_5)_3$ was capable of abstracting fluoride from difluorocyclopropenes but also that highly electrophilic cyclopropenium ions were sufficiently electrophilic to undergo reactions even with weak nucleophiles.

With this insight, we hypothesized that more nucleophilic olefins would also readily add to fluorocyclopropenium ions. Silyl ketene acetals emerged as intriguing reactants because they are more nucleophilic toward cations than arenes.³⁵ Moreover, the formation of $Me_3Si–F$ would provide not only an enthalpic driving force for the reaction but also a means to turn over the triarylborane catalyst. When 3,3-difluoro-1,2-diphenylcyclopropene (**1**) was reacted with silyl ketene acetal **7** (2.2 equiv) and 15 mol % of $B(C_6F_5)_3$ (Table 1, entry 1), we observed nearly full conversion (95% yield) to double alkylation product **8a** by 1H NMR. A brief catalyst screen revealed that many other boranes promoted the reaction. For example, $BF_3\cdot OEt_2$ produced product **8a** in an 87% yield. Triphenylborane (**2b**) produced no product at room temperature; however, heating for 16 h at 50 °C afforded a 72% yield of product **8a**. Other electron-deficient boranes **2c**, **2d**, and **2e** produced **8a** in 76, 91, and 87% yields, respectively. The fluorophilic tri(9-anthrylborane)³⁶ (**2f**) was ineffective in this reaction at 23 °C (Table 1, entry 8). Other Lewis acids such as $TiCl_4$ and $AlCl_3$ gave products in 72 and 92% yields, respectively (Table 1, entries 9 and 10). Trityl tetrakis(pentafluorophenyl)borate gave **8a** in an 81% yield (Table 1, entry 11). Interestingly, trimethylsilyl trifluoromethanesulfonate was ineffective, only producing **8a** in a 6% yield.³⁷

A variety of disubstituted *gem*-difluorocyclopropenes readily undergo double alkylation reactions with silyl ketene acetal **7** (Figure 2). Symmetrical diaryl substrates **1a–1d** gave the corresponding cyclopropene products **8a–8d** bearing two quaternary carbon centers α to the cyclopropene in good to excellent yields. When the reaction using **8a** was conducted on a 1.00 mmol scale, the product was obtained in 75% isolated yield. Unsymmetrical diaryl substrates, such as **1e** and **1f**, also worked well in the reaction, providing the double alkylation products as a mixture of vicinal addition regioisomers. We

Scheme 1. Stoichiometric Reaction of $B(C_6F_5)_3$ and 3,3-Difluoro-1,2-diphenylcyclopropene in C_6D_6 Forms $[Ph_2(C_6D_5)C_3]^+[C_6F_5)_3BF]^-$

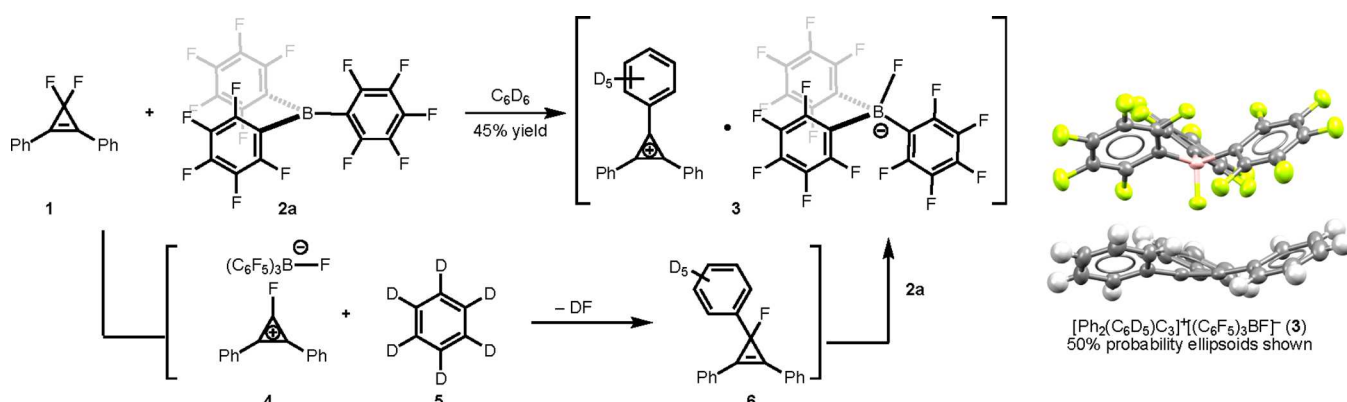
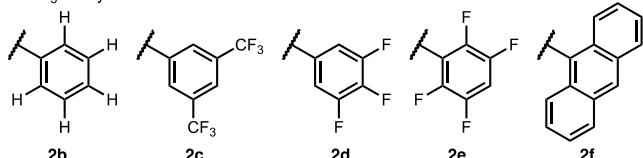


Table 1. Effect of the Catalyst on the C–F Bond Functionalization Reaction^a

Entry	catalyst	¹ H NMR yield 8
1	$B(C_6F_5)_3$	95%
2	none	0%
3	$BF_3 \cdot OEt_2$	87%
4	BPh_3 (2b)	72% ^a
5	2c	76%
6	2d	91%
7	2e	87%
8	$B(9\text{-anthryl})_3$ (2f)	0%
9	$TiCl_4$	72%
10	$AlCl_3$	92%
11	$[Ph_3C]^+[BArF_{20}]^-$ Me_3SiOTf	81%
12		6%

 BAr_3 catalysts. Ar =

^a E = CO_2Et . Yields determined using 1.0 equiv of mesitylene as an internal standard. Standard conditions use 0.15 mmol of compound **1**.

^b 16 h at 50 °C.

noted that the regioselectivity of the addition to the trisubstituted cyclopropenium ions was influenced by their steric and electronic environment. For example, upon cooling the reaction to -25 °C, product **8e** was isolated in an 85% yield as a 3.8:1 mixture of regioisomers, favoring the isomer shown. For the push–pull diaryl substrate **1f**, compound **8f** was produced as the major product by addition of the nucleophile next to the more electron-deficient *p*-cyanophenyl ring (9.2:1 rr) when conducted at 0 °C. Regioselectivity could be increased by further differentiating the substituents on the *gem*-difluorocyclopropenes. Cyclopropene **1g**, bearing an *n*-butyl group, afforded the double alkylation product **8g** in 80% yield as an 8.4:1 mixture of regioisomers at -25 °C, which can be rationalized by a steric effect. Remarkably, cyclopropene **8i** was isolated as a 15:1 mixture of regioisomers in 81% yield. Vicinal double alkylation was exclusively observed in all cases. Presumably, this is due to the phenyl ring being sterically smaller than a tetrasubstituted carbon atom. Finally, when cyclopropene **1j** bearing a benzoate group was tested, the ring-expanded cyclobutene product **9** was isolated in a 51% yield.³⁸

Next, we tested the performance of different silylated nucleophiles on the outcome of the reaction. We synthesized different silyl ketene acetals, silyl enol ethers, and silyl ketene amides bearing different α -substituents to understand the effect of the structure of the nucleophile on the course of the reaction. Using $SiEt_3$ - and $Si(t\text{-}Bu})_2Me_2$ -protected ketene acetals gave **8a** in 82 and 85% ¹H NMR yields, respectively, so the size of the Si group had little effect on the reaction. Silyl ketene amide **10a** and silyl ketene acetal **10b**, each bearing two terminal alkyl groups, gave exclusively the unsymmetrical double addition products **vic-11a** and **vic-11b** in 64 and 93% isolated yields, respectively (Figure 3). Allylsilanes were poor reaction partners in this reaction, affording **gem-11c** resulting

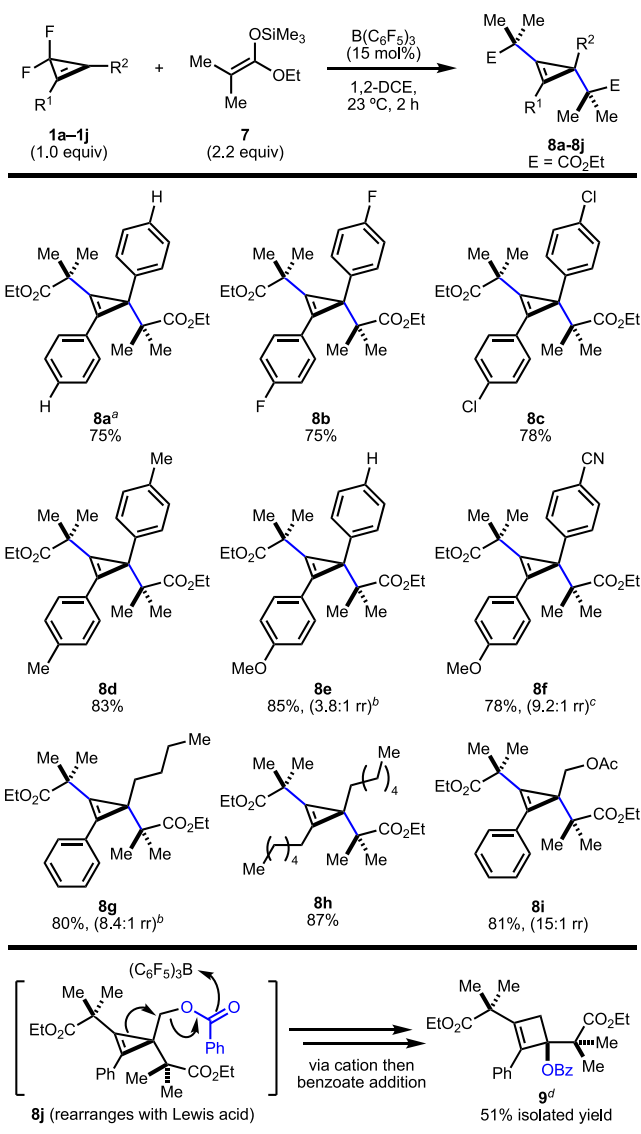


Figure 2. Reaction of silyl ketene acetal **7** with disubstituted *gem*-difluorocyclopropenes (150 μ mol). Regioisomeric ratio based on crude ¹H NMR yields of products using 1.0 equiv of mesitylene as an internal standard. Major regioisomers drawn. ^aRepeated for comparison purposes on a 1.00 mmol scale. ^bReaction performed at -25 °C. ^cReaction performed at 0 °C. ^dReaction performed at -25 °C for 2 h, then warmed to room temperature.

from geminal addition in ~8% yield by ¹H NMR spectroscopic analysis; however, when allyltributylstannane was used as a nucleophile, we isolated compound **gem-11c** in an 88% yield. To our surprise, when 2-trimethylsiloxyfuran was used as a reaction partner, the *gem*-dialkylated cyclopropene regioisomer (**gem-11d**) was formed as a 1:1 mixture of diastereomers (*C*₂/*meso*) in a 79% isolated yield. This observation was confirmed by isolation and X-ray crystallographic analysis of a single crystal of the *C*₂-symmetric diastereomer (Figure 3). Apparently, the small size of the butenolide group promotes geminal addition. With these results, we suspected that α,α -difluoro silyl enol ethers may also result in 1,1-addition product because of the small size and inductively withdrawing nature of the resulting difluoromethylene groups. Indeed, *gem*-difluoromethylenecyclopropene products **gem-11e**, **gem-11f**, and **gem-11g** were isolated as single regioisomers in 63, 71, and 77% yields, respectively (>20:1 selectivity) (Figure 3). The

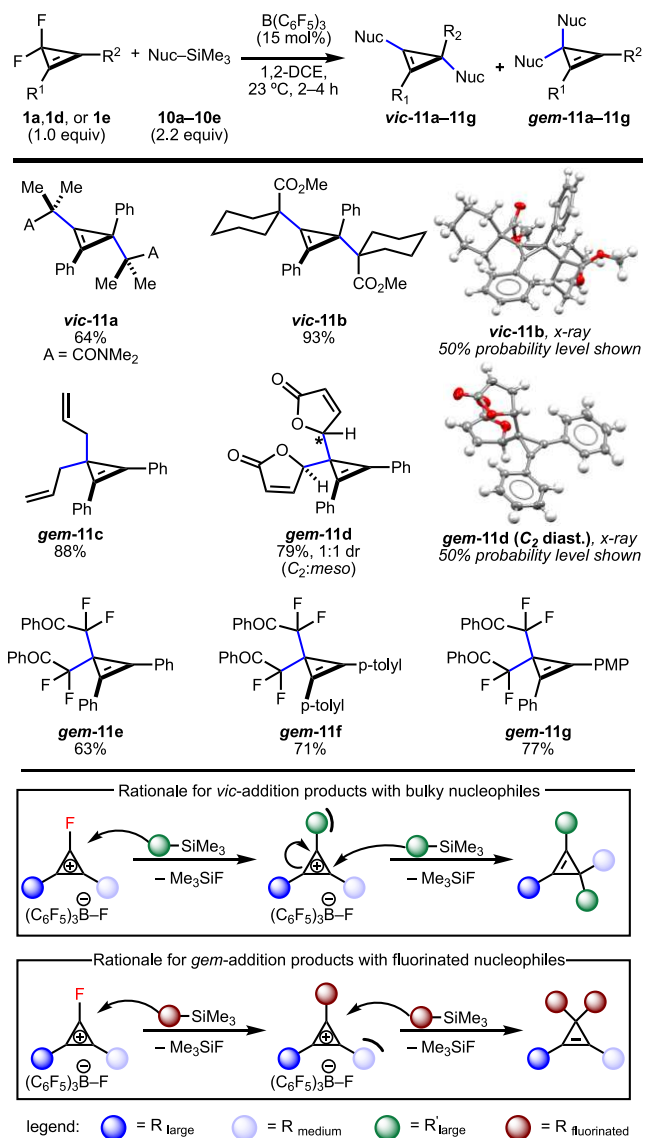
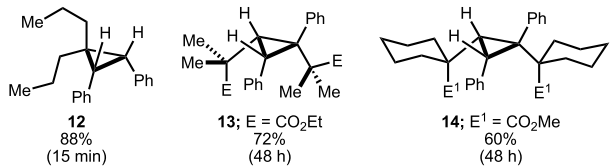


Figure 3. Alkylation of cyclopropenium ions with a variety of silyl-containing nucleophiles. ^aDiastereomeric and regiosomeric ratio based on crude ¹H NMR yields of products using 1.0 equiv of mesitylene as internal standard. Starred carbon indicates an epimeric carbon atom.

connectivity of these compounds was easily established by ¹⁹F NMR analysis, which showed a sharp singlet at $\delta = -92.3$ ppm for compound *gem*-11e.

We next turned our attention to functional group manipulations of the cyclopropene products to obtain orphaned cyclopropanes (Figure 4). Reduction of compound *gem*-11c using 10% Pd/C and H₂ (balloon) afforded *cis*-1,2-diphenyl-3,3-dipropylcyclopropane (**12**) in an 88% isolated yield. Reduction of **8a** proceeded to completion over 2 days, affording **13** as a single diastereomer in a 72% isolated yield. Similarly, the more sterically encumbered cyclopropene *vic*-11b provided the corresponding product **14** in a 60% isolated yield. X-ray crystallographic and (¹H, ¹H)-NOESY data confirmed that the hydrogenation of the cyclopropene compounds occurred from the least sterically encumbered face of the double bond, resulting in cyclopropane products containing two *cis*-*tert*-alkyl groups. Sequential reductions of

Reductions (H₂ (balloon), 10% Pd/C, MeOH)



Stepwise reduction of compound *gem*-11e to fluorinated pyran **15**

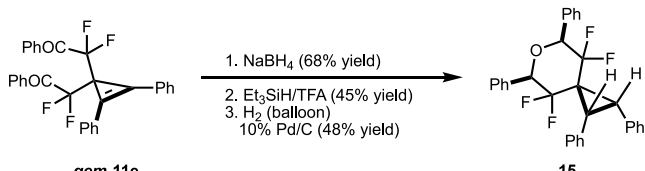


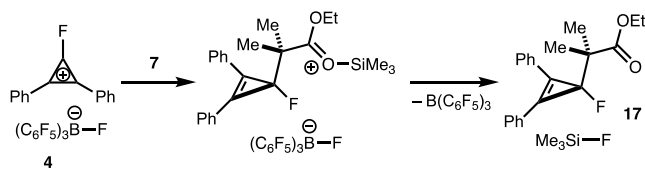
Figure 4. Reduction of cyclopropene substrates to the corresponding orphaned *tert*-alkylcyclopropanes. Reaction times for hydrogenation given in parentheses.

fluorinated compound *gem*-11e proceeded smoothly to afford the fluorinated spirocyclic pyran product **15** over three steps.

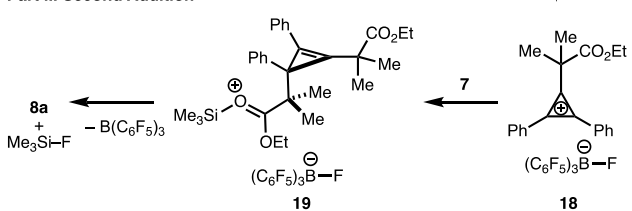
Our proposed mechanism for the transformation is depicted in Scheme 2. In this mechanism, B(C₆F₅)₃ reacts with

Scheme 2. Proposed Mechanism to Obtain *tert*-Alkylcyclopropanes

Part I. First Addition



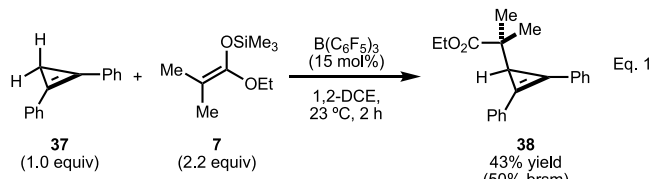
Part II. Second Addition



difluorocyclopropene **1** to afford fluorocyclopropenium ion intermediate **4**. Intermediate **4**, which is stabilized by aromaticity, is also likely stabilized by resonance with the F atom lone pairs because of the overlap of the C 2p and F 2p orbitals. Such effects have been documented in fluorinated cations.³⁹ Next, the nucleophilic silyl ketene acetal **7** reacts with **4** to form a resonance-stabilized oxocarbenium ion **16**. Upon reaction with tris(pentafluorophenyl)fluoroborate, the oxocarbenium ion is desilylated producing Me₃Si–F irreversibly and regenerating B(C₆F₅)₃. The resulting 3-alkyl-3-fluorodiphenylcyclopropane product (**17**) contains a C–F bond that is expected to be more reactive than the C–F bond in the difluorocyclopropene starting material since alkyl groups are electron-donating through hyperconjugation. Thus, a second F atom is readily abstracted producing C-substituted cyclopropenium ion **18**. The resulting cation undergoes a reaction with a second equivalent of nucleophile **7** and

desilylation with the borane catalyst to afford the cyclopropene products.

The ease of the second C–F bond abstraction with $B(C_6F_5)_3$ en route to **8a** was apparent during these studies since we were unable to isolate monofluorinated products like compound **17** under a variety of conditions. For example, we lowered the reaction temperature to $-78\text{ }^\circ\text{C}$ and observed the exclusive formation of **8a**. Therefore, we turned to C–H bond activation of cyclopropene⁴⁰ **37** as a potential method to obtain mono-addition products. When 1,2-diphenylcyclopropene was subjected to the optimized reaction conditions, the incorporation of one equivalent of nucleophile was observed and product **38** was isolated in 43% yield (50% based on recovered starting material) (eq 1). This result can be



rationalized by steric interactions between $B(C_6F_5)_3$ and **38** encountered during a later and more product-like transition structure for the C–H bond abstraction step. Although the cyclopropene C–H bond in **38** is weaker than those in **37**, there is a higher kinetic barrier for the C–H abstraction step with **38**.

To probe the plausibility of this mechanism, we turned to DFT calculations. Specifically, we sought to better understand

the nature of the defluorination steps (*i.e.*, **1** \rightarrow **4** and **17** \rightarrow **18**) since these steps could also conceivably be mediated by Lewis-base-stabilized silyl cations (Figure 5).⁴¹ Using the ω B97X-D/ma-TZVP//SMD(DCE)- ω B97X-D/def2-SV(P) level of theory with the Gaussian 16 C.01 suite of programs,⁴² transition structures for key steps were thoroughly examined *via* constrained conformational searches using the iMTD-GC protocol with CREST using ALPB(CH₂Cl₂)-GFN2-xTB (parameters for DCE not available), followed by full DFT relaxation; quasi-harmonic thermochemical corrections were calculated using the GoodVibes package, and molecular geometries were rendered using Cylview 1.0b.⁴³ NICS(1)_{zz} values were calculated using mPW1PW91/6-311++G(d,p)//SMD(DCE)- ω B97X-D/def2-SV(P),^{42,44} and second-order perturbation theory analysis of the Fock matrix in the NBO basis was performed with SMD(DCE)- ω B97X-D/def2-SV(P) using the NBO 7.0 package and Gaussian16.^{42,45}

The predicted energetically preferred mechanism proceeds as follows (Figure 5): complexation of $B(C_6F_5)_3$ and **1** first leads to reactant complex **IM0**. Subsequent fluoride transfer from **1** to $B(C_6F_5)_3$ through **TS1** ($\Delta G^\ddagger = 15\text{ kcal/mol}$ relative to **1** and $B(C_6F_5)_3$) produces the fluorocyclopropenium fluoroboroborate ion pair **IM1**. Second-order perturbation analysis indicated a strong F(lp) \rightarrow C(cyclopropenium*) interaction stabilizing the fluorocyclopropenium cation intermediate in **IM1** (see the Supporting Information for details). Alkylation of **IM1** with **7** is facile (8 kcal/mol barrier *via* **TS2**) and exceptionally exergonic (by 23 kcal/mol), forming **IM3**, an O-silylated carboxonium triarylfluoroborate ion pair.⁴⁶ Migration of the $[(C_6F_5)_3BF]^-$ counter anion to the backside of the

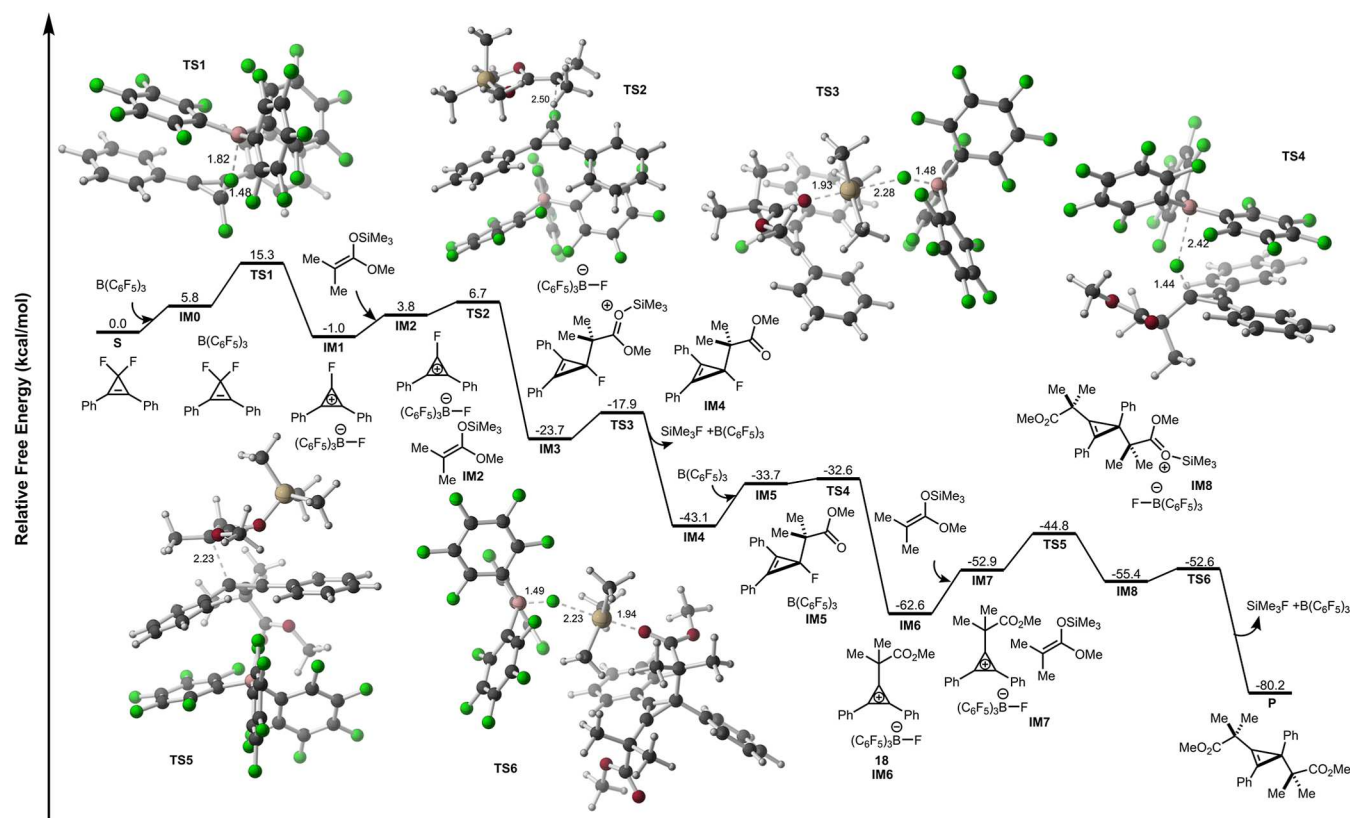


Figure 5. Computed energy profile for the reaction of **1** and **7** catalyzed by **2a** at the ω B97X-D/ma-TZVP//SMD(DCE)- ω B97X-D/def2-SV(P) level. Relative free energies are shown in kcal/mol, and selected distances in optimized transition structures are shown in Å. Et groups in **7** were modeled as Me groups for simplicity. Color code: C, gray; H, white; F, green; O, red; and Si, beige.

silicon in **IM3** (not explicitly modeled here) allows for rapid desilylation by fluoride transfer from $[(C_6F_5)_3BF]^-$ to the silylated oxonium ion through **TS3**, forming **IM4** and Me_3SiF , and regenerating $B(C_6F_5)_3$ ($\Delta G^\ddagger = 6$ kcal/mol, $\Delta G = -19$ kcal/mol). Other desilylation possibilities such as intermolecular fluorine transfer from another molecule of **1** to form **4** and **IM4** ($\Delta G^\ddagger = 16$ kcal/mol) and intramolecular desilylation through fluorine transfer from the cyclopropene motif with a six-membered transition structure to form **IM6** and Me_3SiF ($\Delta G^\ddagger = 14$ kcal/mol) were also considered (see the Supporting Information for details). While these pathways are also kinetically feasible, they are found to be less favorable compared to that *via* **TS3**. Defluorination of **IM4** with $B(C_6F_5)_3$ *via* **TS4** was predicted to be even more facile than that of **1** and irreversible ($\Delta G^\ddagger = 11$ kcal/mol, $\Delta G = -20$ kcal/mol), leading to ion pair **IM6**. Interestingly, **TS4** contains an elongated B–F bond length (2.42 Å), consistent with a very early transition structure for the second fluorine transfer. We believe this early transition structure is reflective of the lability of the C–F bond in intermediates like **17**. Moreover, comparing the NICS(1)_{zz} of the isolated alkylated cyclopropenium cation (-15.7 ppm) from **IM6** and fluorocyclopropenium cation (**IM1** without counter anion, -10.7 ppm) indicated stronger aromaticity of **IM6**. The addition of **7** to **IM6** is predicted to proceed through **TS5** ($\Delta G^\ddagger = 18$ kcal/mol from **IM6**, see the Supporting Information for further discussion on selectivity). Subsequent desilylation in the same fashion as **TS3** through **TS6** afforded the final product with only a small barrier ($\Delta G^\ddagger = 3$ kcal/mol). This process also provided a strong thermodynamic driving force, since it is exergonic by 18 kcal/mol.

In conclusion, we have reported the first example of catalytic C–F bond functionalization of difluorocyclopropenes using $B(C_6F_5)_3$ to form C–C bonds.⁴⁷ The reaction leverages both the stability of aromatic cyclopropenium ions and their reactivity toward silylketene acetals. Our reaction provides fluorinated cyclopropenes and, ultimately, saturated cyclopropanes, which are currently difficult to obtain by traditional methods and would be useful in medicinal chemistry campaigns. We have studied the mechanism of this reaction using quantum chemical calculations, which revealed that the kinetically facile C–F bond abstraction steps are likely mediated by $B(C_6F_5)_3$ and are aided by the formation of aromatic intermediates. Our future directions are aimed at studying the kinetics of this reaction and extending the scope of nucleophiles to enable the synthesis of other orphaned cyclopropanes.

■ ASSOCIATED CONTENT

SI Supporting Information

The Supporting Information is available free of charge at <https://pubs.acs.org/doi/10.1021/jacs.3c05278>.

Experimental details, additional experimental results, and compound characterization (PDF)

Accession Codes

CCDC 2260207, 2260209, and 2260266–2260267 contain the supplementary crystallographic data for this paper. These data can be obtained free of charge via www.ccdc.cam.ac.uk/data_request/cif, or by emailing data_request@ccdc.cam.ac.uk, or by contacting The Cambridge Crystallographic Data Centre, 12 Union Road, Cambridge CB2 1EZ, UK; fax: +44 1223 336033.

■ AUTHOR INFORMATION

Corresponding Author

Sidney M. Wilkerson-Hill – Department of Chemistry, The University of North Carolina at Chapel Hill, Chapel Hill, North Carolina 27599, United States;  orcid.org/0000-0002-4396-5596; Email: smwhill@email.unc.edu

Authors

Joseph P. Mancinelli – Department of Chemistry, The University of North Carolina at Chapel Hill, Chapel Hill, North Carolina 27599, United States

Wang-Yeuk Kong – Department of Chemistry, University of California, Davis, Davis, California 95616, United States;  orcid.org/0000-0002-4592-0666

Wentao Guo – Department of Chemistry, University of California, Davis, Davis, California 95616, United States;  orcid.org/0000-0001-8058-8323

Dean J. Tantillo – Department of Chemistry, University of California, Davis, Davis, California 95616, United States;  orcid.org/0000-0002-2992-8844

Complete contact information is available at:

<https://pubs.acs.org/10.1021/jacs.3c05278>

Notes

The authors declare no competing financial interest.

■ ACKNOWLEDGMENTS

S.M.W.-H. and J.P.M. thank the University of North Carolina, Chapel Hill Chemistry Department for funding. We thank the University of North Carolina's Department of Chemistry NMR Core Laboratory for the use of their NMR spectrometers. This material is based upon work supported by the National Science Foundation under grant nos. CHE-0922858 and CHE-1828183. We thank the University of North Carolina's Department of Chemistry Mass Spectrometry Core Laboratory for their assistance with mass spectrometry analysis. This material is based upon work supported by the National Science Foundation under grant no. CHE-1726291. We thank the University of North Carolina's Department of Chemistry X-ray Crystallography Core and Adam Zahara for single-crystal analysis of **3**, *vic*-**11b**, *gem*-**11c**, and **14**. This material is based upon work supported by the National Science Foundation under grant no. (CHE-2117287). We thank the Aubé group for allowing the use of their IR spectrometer. D.J.T., W.-Y.K., and W.G. gratefully acknowledge support from the National Science Foundation (CHE-1856416 and supercomputing resources from XSEDE and ACCESS program). W.-Y.K. acknowledges the Croucher Foundation for continued financial support through a doctoral scholarship.

■ REFERENCES

- (1) (a) Talele, T. T. The “Cyclopropyl Fragment” is a Versatile Player that Frequently Appears in Preclinical/Clinical Drug Molecules. *J. Med. Chem.* 2016, 59, 8712–8756. (b) Shearer, J.; Castro, J. L.; Lawson, A. D. G.; MacCoss, M.; Taylor, R. D. Rings in Clinical Trials and Drugs: Present and Future. *J. Med. Chem.* 2022, 65, 8699–8712.
- (2) Bien, J.; Davulcu, A.; DelMonte, A. J.; Fraunhoffer, K. J.; Gao, Z.; Hang, C.; Hsiao, Y.; Hu, W.; Katipally, K.; Littke, A.; Pedro, A.; Qiu, Y.; Sandoval, M.; Schild, R.; Soltani, M.; Tedesco, A.; Vanyo, D.; Vemishetti, P.; Waltermire, R. E. The First Kilogram Synthesis of Beclabuvir, an HCV NSSB Polymerase Inhibitor. *Org. Process Res. Dev.* 2018, 22, 1393–1408.

(3) Segal-Maurer, S.; DeJesus, E.; Stellbrink, H.-J.; Castagna, A.; Richmond, G. J.; Sinclair, G. I.; Siripassorn, K.; Ruane, P. J.; Berhe, M.; Wang, H.; Margot, N. A.; Dvory-Sobel, H.; Hyland, R. H.; Brainard, D. M.; Rhee, M. S.; Baeten, J. M.; Molina, J.-M. Capsid Inhibition with Lenacapavir in Multidrug-Resistant HIV-1 Infection. *N. Engl. J. Med.* **2022**, *386*, 1793–1803.

(4) Allais, C.; Connor, C. G.; Do, N. M.; Kulkarni, S.; Lee, J. W.; Lee, T.; McInturff, E.; Piper, J.; Place, D. W.; Ragan, J. A.; Weekly, R. M. Development of the Commercial Manufacturing Process for Nirmatrelvir in 17 Months. *ACS Cent. Sci.* **2023**, *9*, 849–857.

(5) Eng, H.; Dantonio, A. L.; Kadar, E. P.; Obach, R. S.; Di, L.; Lin, J.; Patel, N. C.; Boras, B.; Walker, G. S.; Novak, J. J.; Kimoto, E.; Singh, R. S. P.; Kalgutkar, A. S. Disposition of PF-07321332 (Nirmatrelvir), an Orally Bioavailable Inhibitor of SARS-CoV-2 3CL Protease, across Animals and Humans. *Drug Metab. Dispos.* **2022**, *50*, 576–590.

(6) For strategies to obtain *tert*-alkylcyclopropanes using carbocyclization reactions, see: (a) Kubota, K.; Isaka, M.; Nakamura, M.; Nakamura, E. Ligand Control in the Stereoselective Allylzincation of Cyclopropenes. *J. Am. Chem. Soc.* **1993**, *115*, 5867–5868. (b) Nakamura, M.; Arai, M.; Nakamura, E. Carbometallation of Cyclopropene. Ligand-Induced Enantioselective Allylzincation. *J. Am. Chem. Soc.* **1995**, *117*, 1179–1180. (c) Nakamura, E.; Kubota, K. Carbometallation of Cyclopropene. Diastereoselective *cis*-Addition of Zincated Amides, Esters, and Hydrazones. *J. Org. Chem.* **1997**, *62*, 792–793. (d) Nakamura, M.; Inoue, T.; Sato, A.; Nakamura, E. Asymmetric Construction of Quaternary Carbon Centers by Regio- and Enantiocontrolled Allylzincation. *Org. Lett.* **2000**, *2*, 2193–2196.

(7) (a) Lebel, H.; Marcoux, J. -F.; Molinaro, C.; Charette, A. B. Stereoselective Cyclopropanation Reactions. *Chem. Rev.* **2003**, *103*, 977–1050. (b) Roy, M. N.; Lindsay, V. N. G.; Charette, A. B. Cyclopropanation Reactions (Chapter 1.14). In *Science of Synthesis: Stereoselective Reactions of Carbon–Carbon Double Bonds*; de Vries, J., Ed.; Georg Thieme Verlag KG: New York, 2011; pp 731–817. (c) Chen, D. Y.-K.; Pouwer, R. H.; Richard, J.-A. Recent advances in the Total Synthesis of Cyclopropane-Containing Natural Products. *Chem. Soc. Rev.* **2012**, *41*, 4631–4642. (d) Kulinkovich, O. G. *Cyclopropanes in Organic Synthesis*; Wiley: Hoboken, NJ, 2015; pp 57–98. (e) Ebner, C.; Carreira, E. M. Cyclopropanation Strategies in Recent Total Syntheses. *Chem. Rev.* **2017**, *117*, 11651–11679. (f) Wu, W.; Lin, Z.; Jiang, H. Recent Advances in the Synthesis of Cyclopropanes. *Org. Biomol. Chem.* **2018**, *16*, 7315–7329.

(8) Charette, A. B.; Beauchemin, A. Simmons-Smith Cyclopropanation Reaction. In *Organic Reactions*; Overman, L. E., Ed.; Wiley, 2001; Vol. 58, pp 7–11.

(9) Doyle, M. P.; McKervey, M. A.; Ye, T. *Modern Catalytic Methods for Organic Synthesis with Diazo Compounds: From Cyclopropanes to Ylides*; Wiley: New York, 1998; pp 163–275.

(10) (a) Kirmse, W.; Koppannia, S. Stereochemistry of Carbenic 1,2-Vinyl Shifts. *J. Org. Chem.* **1998**, *63*, 1178–1184. (b) Crone, B.; Kirsch, S. 1,2-Alkyl Migration as a Key Element in the Invention of Cascade Reactions Catalyzed by π -Acids. *Chem.—Eur. J.* **2008**, *14*, 3514–3522.

(11) Griller, D.; Ingold, K. U. Free-Radical Clocks. *Acc. Chem. Res.* **1980**, *13*, 317–323.

(12) (a) Ritchie, N. F. C.; Zahara, A. J.; Wilkerson-Hill, S. M. Divergent Reactivity of α,α -Disubstituted Alkenyl Hydrazones: Bench Stable Cyclopropylcarbinyl Equivalents. *J. Am. Chem. Soc.* **2022**, *144*, 2101–2106. (b) Johnson, J. D.; Teebles, C. R.; Akkawi, N. R.; Wilkerson-Hill, S. M. Efficient Synthesis of Orphaned Cyclopropanes using Sulfones as Carbene Equivalents. *J. Am. Chem. Soc.* **2022**, *144*, 14471–14476.

(13) Wang, F.; Luo, T.; Hu, J.; Wang, Y.; Krishnan, H. S.; Jog, P. V.; Ganesh, S. K.; Prakash, G. K. S.; Olah, G. A. Synthesis of *gem*-Difluorinated Cyclopropanes and Cyclopropenes: Trifluoromethyltrimethylsilane as a Difluorocarbene Source. *Angew. Chem., Int. Ed.* **2011**, *50*, 7153–7157.

(14) Nosik, P. S.; Pashko, M. O.; Poturai, A. S.; Kvasha, D. A.; Pashenko, A. E.; Rozhenko, A. B.; Suikov, S.; Volochnyuk, D. M.; Ryabukhin, S. V.; Yagupolskii, Y. L. Monosubstituted 3,3-Difluorocyclopropenes as Bench-Stable Reagents: Scope and Limitations. *Eur. J. Org. Chem.* **2021**, 6604–6615.

(15) Li, L.; Ni, C.; Wang, F.; Hu, J. Deoxyfluorination of Alcohols with 3,3-difluoro-1,2-diarylcyclopropenes. *Nat. Commun.* **2016**, *7*, 13320.

(16) (a) Sargeant, P. B.; Krespan, C. G. Fluorocyclopropanes II. Synthesis, Properties, and Reactions of Perfluorocyclopropene. *J. Am. Chem. Soc.* **1969**, *91*, 415–419. (b) Law, D. C.; Tobey, S. W.; West, R. Fluorinated cyclopropenes and cyclopropenium ions. *J. Org. Chem.* **1973**, *38*, 768–773. (c) Smart, B. E. Fluorinated Cyclopropenyl Methyl Ethers. New Stable Cyclopropenium Cations. *J. Org. Chem.* **1976**, *41*, 2377–2379. (d) Craig, N. C.; Fleming, G. F.; Pranata, J. Vibrational Spectra and Force Constants for the Perfluorocyclopropenyl Cation. *J. Am. Chem. Soc.* **1985**, *107*, 7324–7329.

(17) (a) Breslow, R.; Hover, H.; Chang, H. W. The Synthesis and Stability of some Cyclopropenium Ions with Alkyl Substituents. *J. Am. Chem. Soc.* **1962**, *84*, 3168–3174. (b) Padwa, A.; Chou, C. S. Effects of Substituents on the Type II Photoreaction of Tetrasubstituted Cyclopropenes. *Tetrahedron* **1981**, *37*, 3269–3274. (c) Padwa, A.; Goldstein, S. I.; Rosenthal, R. J. Single-Electron-Transfer Pathway in the Coupling of Cyclopropenyl Cations with Organometallic Reagents. *J. Org. Chem.* **1987**, *52*, 3278–3285.

(18) (a) For a review on catalytic reactions of cyclopropenium ions, see: Wilson, R. M.; Lambert, T. H. Cyclopropenium Ions in Catalysis. *Acc. Chem. Res.* **2022**, *55*, 3057–3069. (b) For recent examples of C–C bond formation to cyclopropenium ions, see: Tu, H.-F.; Jeandin, A.; Suero, M. G. Catalytic Synthesis of Cyclopropenium Cations with Rh-Carbonyoids. *J. Am. Chem. Soc.* **2022**, *144*, 16737–16743.

(19) Corey, E. J.; Posner, G. H. Selective Formation of Carbon–Carbon Bonds between Unlike Groups using Organocopper Reagents. *J. Am. Chem. Soc.* **1967**, *89*, 3911–3912.

(20) (a) Rubin, M.; Rubina, M.; Gevorgyan, V. Transition Metal Chemistry of Cyclopropenes and Cyclopropanes. *Chem. Rev.* **2007**, *38*, 3117–3179. (b) Sekine, K.; Ushiyama, A.; Endo, Y.; Mikami, K. Enantioselective Functionalization of Difluorocyclopropenes Catalyzed by Chiral Copper Complexes: Proposal for Chiral *gem*-Dimethyl and *tert*-Butyl Analogues. *J. Org. Chem.* **2020**, *85*, 7916–7924. (c) Adekenova, K. S.; Wyatt, P. B.; Adekenov, S. M. The Preparation and Properties of 1,1-difluorocyclopropane Derivatives. *Beilstein J. Org. Chem.* **2021**, *17*, 245–272. (d) Vicente, R. C–C Bond Cleavages of Cyclopropenes: Operating for Selective Ring-Opening Reactions. *Chem. Rev.* **2021**, *121*, 162–226. (e) Cohen, Y.; Marek, I. Regio- and Diastereoselective Carbometalation Reaction of Cyclopropenes. *J. Am. Chem. Soc.* **2022**, *55*, 2848–2868. (f) Zhang, Z.; Gevorgyan, V. Palladium Hydride-Enabled Hydroalkenylation of Strained Molecules. *J. Am. Chem. Soc.* **2022**, *144*, 20875–20883. (g) Sekine, K.; Akaishi, D.; Konagaya, K.; Ito, S. Copper-Catalyzed Enantioselective Hydro-silylation of *gem*-Difluorocyclopropenes Leading to a Stereochemical Study of the Silylated *gem*-Difluorocyclopropanes. *Chem.—Eur. J.* **2022**, *28*, No. e202200657. (h) Wang, M.; Simon, J. C.; Xu, M.; Corio, S. A.; Hirschi, J. S.; Dong, V. M. Copper-Catalyzed Hydroamination: Enantioselective Addition of Pyrazoles to Cyclopropenes. *J. Am. Chem. Soc.* **2023**, *145*, 14573–14580.

(21) Yamani, K.; Pierre, H.; Archambeau, A.; Meyer, C.; Cossy, J. Asymmetric Transfer Hydrogenation of *gem*-Difluorocyclopropenyl Esters: Access to Enantioenriched *gem*-Difluorocyclopropanes. *Angew. Chem., Int. Ed.* **2020**, *59*, 18505–18509.

(22) (a) For reviews on borane catalysis, see: Lawson, J. R.; Melen, R. L. Tris(pentafluorophenyl)borane and Beyond: Modern Advances in Borylation Chemistry. *Inorg. Chem.* **2017**, *56*, 8627–8643. (b) Carden, J. L.; Dasgupta, A.; Melen, R. L. Halogenated Triarylboranes: Synthesis Properties and Applications in Catalysis. *Chem. Soc. Rev.* **2020**, *49*, 1706–1725. (c) Kumar, G.; Roy, S.; Chatterjee, I. Tris(pentafluorophenyl)borane catalyzed C–C and C–Heteroatom Bond Formation. *Org. Biomol. Chem.* **2021**, *19*, 1230–1267.

(23) (a) Jacobsen, H.; Berke, H.; Doring, S.; Kehr, G.; Erker, G.; Frohlich, R.; Meyer, O. Lewis acid properties of Tris-

(pentafluorophenyl)borane. Structure and Bonding in L-B(C₆F₅)₃ complexes. *Organometallics* **1999**, *18*, 1724–1735. (b) Beckett, M. A.; Brassington, D. S.; Coles, S. J.; Hursthouse, M. B. Lewis Acidity of Tris(pentafluorophenyl)borane: Crystal and Molecular structure of B(C₆F₅)₃•OPEt₃. *Inorg. Chem. Commun.* **2000**, *3*, 530–533.

(24) For examples of cyclopropane synthesis leveraging the Lewis acidity of boron, see: (a) Dasgupta, A.; Babaahmadi, R.; Slater, B.; Yates, B. F.; AriaFard, A.; Melen, R. L. Borane-Catalyzed Stereoselective C–H Insertion, Cyclopropanation, and Ring-Opening Reactions. *Chem.* **2020**, *6*, 2364–2381. (b) Mancinelli, J. P.; Wilkerson-Hill, S. M. Tris(pentafluorophenyl)borane-Catalyzed Cyclopropanation of Styrenes with Aryldiazoacetates. *ACS Catal.* **2020**, *10*, 11171–11176.

(25) (a) Krossing, I.; Raabe, I. Relative Stabilities of Weakly Coordinating Anions: A Computational Study. *Chem.—Eur. J.* **2004**, *10*, 5017–5030. (b) Müller, L. O.; Himmel, D.; Stauffer, J.; Steinfeld, G.; Slattery, J.; Santiso-Quiñones, G.; Brecht, V.; Krossing, I. Simple Access to the Non-Oxidizing Lewis Superacid PhF→Al(OR^F)₃ (R^F = C(CF₃)₃). *Angew. Chem., Int. Ed.* **2008**, *47*, 7659–7663. (c) Erdmann, P.; Leitner, J.; Schwarz, J.; Greb, L. An Extensive Set of Accurate Fluoride Ion Affinities for p-Block Element Lewis Acids and Basic Design Principles for Strong Fluoride Ion Acceptors. *ChemPhysChem* **2020**, *21*, 987–994.

(26) (a) For reviews, see: Stahl, T.; Klare, H. F. T.; Oestreich, M. Main-Group Lewis Acids for C–F Bond Activation. *ACS Catal.* **2013**, *3*, 1578–1587. (b) Ćorković, A.; Dorian, A.; Williams, F. J. Improvements in Efficiency and Selectivity for C–F Bond Halogen Exchange Reactions by Using Boron Reagents. *Synlett* **2023**, *34*, 193–202.

(27) Willcox, D. R.; Nichol, G. S.; Thomas, S. P. Borane-catalyzed C(sp³)-F Bond Arylation and Esterification Enabled by Transboraylation. *ACS Catal.* **2021**, *11*, 3190–3197.

(28) For C–F bond activation in glycosides, see: (a) Sati, G. C.; Martin, J. L.; Xu, Y.; Malakar, T.; Zimmerman, P. M.; Montgomery, J. Fluoride Migration Catalysis Enables Simple, Stereoselective, and Iterative Glycosylation. *J. Am. Chem. Soc.* **2020**, *142*, 7235–7242. (b) For the recent applications to polymerize sugars, see: Wu, L.; Zhou, Z.; Sathe, D.; Zhou, J.; Dym, S.; Zhao, Z.; Wang, J.; Niu, J. Precision Native Polysaccharides from Living Polymerization of Anhydrosugars. *Nat. Chem.* **2023**, DOI: 10.1038/s41557-023-01193-2.

(29) Mandal, D.; Gupta, R.; Jaiswal, A. K.; Young, R. D. Frustrated Lewis-Pair-Mediated Selective Single Fluoride Substitution in Trifluoromethyl Groups. *J. Am. Chem. Soc.* **2020**, *142*, 2572–2578.

(30) Wang, J.; Ogawa, Y.; Shibata, N. Activation of Saturated Fluorocarbons to Synthesize Spirobiindanes, Monofluoroalkenes, and Indane Derivatives. *iScience* **2019**, *17*, 132–143.

(31) McKnight, E. A.; Arora, R.; Pradhan, E.; Fujisato, Y. H.; Ajayi, A. J.; Lautens, M.; Zeng, T.; Le, C. M. BF₃–Catalyzed Intramolecular Fluorocarbonylation of Alkynes via Halide Recycling. *J. Am. Chem. Soc.* **2023**, *145*, 11012–11018.

(32) Köring, L.; Stepen, A.; Birenheide, B.; Barth, S.; Leskov, M.; Schoch, R.; Krämer, F.; Breher, F.; Paradies, J. Boron-Centered Lewis Superacid through Redox-Active Ligands: Application in C–F and S–F Bond Activation. *Angew. Chem., Int. Ed.* **2023**, *62*, No. e202216959.

(33) Fuchibe, K.; Hatta, H.; Oh, K.; Oki, R.; Ichikawa, J. Lewis Acid Promoted Single C–F Bond Activation of the CF₃ Group: S_N1'-Type 3,3-Difluoroallylation of Arenes with 2-Trifluoromethyl-1-alkenes. *Angew. Chem., Int. Ed.* **2017**, *56*, 5890–5893.

(34) Breslow, R. Synthesis of the s-Triphenylcyclopropenyl Cation. *J. Am. Chem. Soc.* **1957**, *79*, 5318.

(35) Mayr's Database of Reactivity Parameters, AK Prof. Mayr. <https://www.cup.lmu.de/oc/mayr/reaktionsdatenbank/> (accessed Jan 23, 2023).

(36) Yamaguchi, S.; Akiyama, S.; Tamao, K. Colorimetric Fluoride Ion Sensing by Boron-Containing π -Electron Systems. *J. Am. Chem. Soc.* **2001**, *123*, 11372–11375.

(37) The effects of solvent, temperature, time, and other variables were also tested and are described in the *Supporting Information*.

(38) Breslow, R.; Lockhart, J.; Small, A. The Cyclopropenyl Cation, a Non-Classical Carbonium Ion. *J. Am. Chem. Soc.* **1962**, *84*, 2793–2800.

(39) Olah, G. A.; Prakash, G. K. S.; Rasul, G. Study of the Fluoro- and Chlorodimethylbutyl Cations. *Proc. Natl. Acad. Sci. U.S.A.* **2013**, *110*, 8427–8430.

(40) Zimmerman, H. E.; Wright, C. W. Triplet Photochemistry of Acyl and Imino Cyclopropenes. A Rearrangement to Afford Furans and Pyrroles: Reaction and Mechanism. *J. Am. Chem. Soc.* **1992**, *114*, 6603–6613.

(41) Klare, H. F. T.; Albers, L.; Süss, L.; Keess, S.; Müller, T.; Oestreich, M. Silylum Ions: From Elusive Reactive Intermediates to Potent Catalysts. *Chem. Rev.* **2021**, *121*, 5889–5985.

(42) (a) Chai, J. D.; Head-Gordon, M. Long-Range Corrected Hybrid Density Functionals with Damped Atom–Atom Dispersion Corrections. *Phys. Chem. Chem. Phys.* **2008**, *10*, 6615–6620. (b) Zheng, J.; Xu, X.; Truhlar, D. G. Minimally Augmented Karlsruhe Basis Sets. *Theor. Chem. Acc.* **2011**, *128*, 295–305. (c) Marenich, A. V.; Cramer, C. J.; Truhlar, D. G. Universal Solvation Model Based on Solute Electron Density and on a Continuum Model of the Solvent Defined by the Bulk Dielectric Constant and Atomic Surface Tensions. *J. Phys. Chem. B* **2009**, *113*, 6378–6396. (d) Weigend, F.; Ahlrichs, R. Balanced Basis Sets of Split Valence, Triple Zeta Valence and Quadruple Zeta Valence Quality for H to Rn: Design and Assessment of Accuracy. *Phys. Chem. Chem. Phys.* **2005**, *7*, 3297–3305. Frisch, M. J.; Trucks, G. W.; Schlegel, H. B.; Scuseria, G. E.; Robb, M. A.; Cheeseman, J. R.; Scalmani, G.; Barone, V.; Petersson, G. A.; Nakatsuji, H.; Li, X.; Caricato, M.; Marenich, A. V.; Bloino, J.; Janesko, B. G.; Gomperts, R.; Mennucci, B.; Hratchian, H. P.; Ortiz, J. V.; Izmaylov, A. F.; Sonnenberg, J. L.; Williams-Young, D.; Ding, F.; Lipparini, F.; Egidi, F.; Goings, J.; Peng, B.; Petrone, A.; Henderson, T.; Ranasinghe, D.; Zakrzewski, V. G.; Gao, J.; Rega, N.; Zheng, G.; Liang, W.; Hada, M.; Ehara, M.; Toyota, K.; Fukuda, R.; Hasegawa, J.; Ishida, M.; Nakajima, T.; Honda, Y.; Kitao, O.; Nakai, H.; Vreven, T.; Throssell, K.; Montgomery, J. A., Jr.; Peralta, J. E.; Ogliaro, F.; Bearpark, M. J.; Heyd, J. J.; Brothers, E. N.; Kudin, K. N.; Staroverov, V. N.; Keith, T. A.; Kobayashi, R.; Normand, J.; Raghavachari, K.; Rendell, A. P.; Burant, J. C.; Iyengar, S. S.; Tomasi, J.; Cossi, M.; Millam, J. M.; Klene, M.; Adamo, C.; Cammi, R.; Ochterski, J. W.; Martin, R. L.; Morokuma, K.; Farkas, O.; Foresman, J. B.; Fox, D. J. *Gaussian 16*, Revision C.01; Gaussian, Inc.: Wallingford CT, 2016.

(43) (a) Pracht, P.; Bohle, F.; Grimme, S. Automated Exploration of the Low-Energy Chemical Space with Fast Quantum Chemical Methods. *Phys. Chem. Chem. Phys.* **2020**, *22*, 7169–7192. (b) Ehlert, S.; Stahn, M.; Spicher, S.; Grimme, S. Robust and Efficient Implicit Solvation Model for Fast Semiempirical Methods. *J. Chem. Theory Comput.* **2021**, *17*, 4250–4261. (c) Bannwarth, C.; Ehlert, S.; Grimme, S. GFN2-xTB—An Accurate and Broadly Parametrized Self-Consistent Tight-Binding Quantum Chemical Method with Multipole Electrostatics and Density-Dependent Dispersion Contributions. *J. Chem. Theory Comput.* **2019**, *15*, 1652–1671. (d) Grimme, S. Supramolecular Binding Thermodynamics by Dispersion-Corrected Density Functional Theory. *Chem.—Eur. J.* **2012**, *18*, 9955–9964. (e) Luchini, G.; Alegre-Requena, J. V.; Funes-Ardoiz, I.; Paton, R. S. GoodVibes: Automated Thermochemistry for Heterogeneous Computational Chemistry Data. *F1000Research* **2020**, *9*, 291. (f) Legault, C. Y. *CYLview, 1.0b*; Université de Sherbrooke, 2009.

(44) (a) Adamo, C.; Barone, V. Exchange functionals with improved long-range behavior and adiabatic connection methods without adjustable parameters: The mPW and mPW1PW models. *J. Chem. Phys.* **1998**, *108*, 664–675. (b) Frisch, M. J.; Pople, J. A.; Binkley, J. S. Self-Consistent Molecular Orbital Methods 25. Supplementary Functions for Gaussian Basis Sets. *J. Chem. Phys.* **1984**, *80*, 3265–3269. (c) Franc, M. M.; Pietro, W. J.; Hehre, W. J.; Binkley, J. S.; Gordon, M. S.; DeFrees, D. J.; Pople, J. A. Self-Consistent Molecular Orbital Methods. XXIII. A Polarization-Type Basis Set for Second-Row Elements. *J. Chem. Phys.* **1982**, *77*, 3654–3665. (d) Schleyer, P. v R.; Maerker, C.; Dransfeld, A.; Jiao, H.; van Eikema Hommes, N. J. R. Nucleus Independent Chemical Shifts: A Simple and Efficient

Aromaticity Probe. *J. Am. Chem. Soc.* **1996**, *118*, 6317–6318.
(e) Fowler, P. W.; Steiner, E.; Zanasi, R.; Cadioli, B. Electric and Magnetic Properties of Hexaethynylbenzene. *Mol. Phys.* **1999**, *96*, 1099–1108. (f) Steiner, E.; Fowler, P. W.; Jenneskens, L. W. Counter-Rotating Ring Currents in Coronene and Corannulene. *Angew. Chem., Int. Ed.* **2001**, *40*, 362–366.

(45) Glendening, E. D.; Landis, C. R.; Weinhold, F. NBO 7.0: New Vistas in Localized and Delocalized Chemical Bonding Theory. *J. Comput. Chem.* **2019**, *40*, 2234–2241.

(46) For the preparation and characterization of stable silylated carboxonium ions, see: Prakash, G. K. S.; Bae, C.; Rasul, G.; Olah, G. A. Preparation and NMR Study of Silylated Carboxonium Ions. *J. Org. Chem.* **2002**, *67*, 1297–1301.

(47) For an example which proceeds through the cyclopropenone, see: Wang, T.; Chen, J.; Shi, Y. S.; Liu, X. X.; Guo, L.; Wu, Y. Synthesis of Functional Carbocycles and Heterocycles via Transition-Metal-Catalyzed Annulation or Homocoupling of Difluorocyclopropanes. *Tetrahedron Lett.* **2022**, *99*, 153845.

□ Recommended by ACS

Ferrocenium Boronic Acid Catalyzed Deoxygenative Coupling of Alcohols with Carbon- and Nitrogen-Based Borate and Silane Nucleophiles

Jake J. Blackner, J. Adam McCubbin, *et al.*

JUNE 07, 2023

THE JOURNAL OF ORGANIC CHEMISTRY

READ 

Nickel-Catalyzed Exhaustive Hydrodefluorination of Perfluoroalkyl Arenes

Ryohei Doi, Sensuke Ogoshi, *et al.*

MAY 04, 2023

JOURNAL OF THE AMERICAN CHEMICAL SOCIETY

READ 

Lithium Aryltrifluoroborate as a Catalyst for Halogen Transfer

Kengo Inoue, Kentaro Okano, *et al.*

MARCH 03, 2023

ACS CATALYSIS

READ 

Three-Component Approach to Densely Functionalized Trifluoromethyl Allenols by Asymmetric Organocatalysis

Marie Deliaval, Kálmán J. Szabó, *et al.*

APRIL 26, 2023

JOURNAL OF THE AMERICAN CHEMICAL SOCIETY

READ 

[Get More Suggestions >](#)

Correction to “Borane-Catalyzed C–F Bond Functionalization of *gem*-Difluorocyclopropenes Enables the Synthesis of Orphaned Cyclopropanes”

Joseph P. Mancinelli, Wang-Yeuk Kong, Wentao Guo, Dean J. Tantillo, and Sidney M. Wilkerson-Hill*

J. Am. Chem. Soc. 2023, 145 (31), 17389–17397. DOI: 10.1021/jacs.3c05278



Cite This: *J. Am. Chem. Soc.* 2023, 145, 24434–24435



Read Online

ACCESS |

Metrics & More

Article Recommendations

Supporting Information

Page 17393 and Section VIII of the [Supporting Information](#): The solvation model used to calculate the values in Figure 5 and the [Supporting Information](#) was reported incorrectly. The IEF-PCM solvation model¹ was used throughout the study and not the SMD model² as originally reported. This error does not affect the conclusions drawn in the computational section. We apologize for the error.

- Article Page 17393: The corrected article text should read: Using the ω B97X-D/ma-TZVP//IEF-PCM(DCE)- ω B97X-D/def2-SV(P) level of theory with the *Gaussian16 C.01* suite of programs,⁴² transition structures for key steps were thoroughly examined via constrained conformational searches using the iMTD-GC protocol with CREST using ALPB(CH_2Cl_2)-GFN2-xTB (parameters for DCE not available), followed by full DFT relaxation; quasi-harmonic thermochemical corrections were calculated using the *GoodVibes* package, and molecular geometries were rendered using *Cylview 1.0b*.⁴³ NICS(1)_{zz} values were calculated using mPW1PW91/6-311++G(d,p)//IEF-PCM(DCE)- ω B97X-D/def2-SV(P),^{42,44} and second-order perturbation theory analysis of the Fock matrix in the NBO basis were performed with IEF-PCM(DCE)- ω B97X-D/def2-SV(P) using the NBO 7.0 package and *Gaussian16*.^{42,45}
- Article Page 17393: The corrected Figure 5 caption should read: Computed energy profile for the reaction of **1** and **7** catalyzed by **2a** at the ω B97X-D/ma-TZVP//IEF-PCM(DCE)- ω B97X-D/def2-SV(P) level. Relative free energies are shown in kcal/mol, and selected distances in optimized transition structures are shown in Å. Et groups in **7** were modeled as Me groups for simplicity. Color code: C, gray; H, white; F, green; O, red; Si, beige.
- Reference 42c should read: Cancès, E.; Mennucci, B.; Tomasi, B. A new integral equation formalism for the polarizable continuum model: Theoretical background and applications to isotropic and anisotropic dielectrics. *J. Chem. Phys.* 1997, 107, 3032–3041.

The revised [Supporting Information](#) includes the following changes:

- Page S57: Solvation effects were considered by the IEF-PCM solvation model in dichloroethane.³⁰ The final free

energy is evaluated according to the following equation: $G_{\text{final}} = G_{\text{corr}} + E_{\text{solv,low}} - E_{\text{gas,low}} + E_{\text{gas,high}}$ where G_{corr} is the free energies correction with IEF-PCM(DCE)- ω B97X-D/def2-SV(P) level of theory, $+ E_{\text{solv,low}} - E_{\text{gas,low}}$ is the solvation free energy obtained from difference of gas phase and solution phase electronic energies at ω B97X-D/def2-SV(P) level of theory, and $E_{\text{gas,high}}$ is the gas phase single point electronic energy at ω B97X-D/ma-TZVP level of theory.

- Page S58 2. **Table S14**: Electronic energies and free energy corrections (in Hartrees) calculated at ω B97X-D/ma-TZVP//IEF-PCM(DCE)- ω B97X-D/def2-SV(P) level of theory.
- Page S61: NICS(1)_{zz} values were calculated using mPW1PW91/6-311++G(d,p)//IEF-PCM(DCE)- ω B97X-D/def2-SV(P) level of theory.
- Page S65: **Table S15**. Electronic energies and free energy corrections (in Hartrees) calculated at ω B97X-D/ma-TZVP//IEF-PCM(DCE)- ω B97X-D/def2-SV(P) level of theory.
- Reference 30: Cancès, E.; Mennucci, B.; Tomasi, B. A new integral equation formalism for the polarizable continuum model: Theoretical background and applications to isotropic and anisotropic dielectrics. *J. Chem. Phys.* 1997, 107, 3032–3041.

A revised [Supporting Information](#) file has been included to reflect these changes:

ASSOCIATED CONTENT

Supporting Information

The Supporting Information is available free of charge at <https://pubs.acs.org/doi/10.1021/jacs.3c09124>.

Experimental details, additional experimental results, and compound characterization ([PDF](#))

Published: October 24, 2023



ACS Publications

© 2023 American Chemical Society

24434

<https://doi.org/10.1021/jacs.3c09124>
J. Am. Chem. Soc. 2023, 145, 24434–24435

■ REFERENCES

(1) Cancès, E.; Mennucci, B.; Tomasi, B. A new integral equation formalism for the polarizable continuum model: Theoretical background and applications to isotropic and anisotropic dielectrics. *J. Chem. Phys.* **1997**, *107*, 3032–3041.

(2) Marenich, A. V.; Cramer, C. J.; Truhlar, D. G. Universal Solvation Model Based on Solute Electron Density and on a Continuum Model of the Solvent Defined by the Bulk Dielectric Constant and Atomic Surface Tensions. *J. Phys. Chem. B* **2009**, *113*, 6378–6396.